

Measuring Ozone via Satellite: Direct Detection vs. Photolysis Proxy Measurements in the Infrared, by Daniel Carpenter

Project Advisor: Dr. Martin Mlynchak (NASA Langley)

Glossary of Acronyms

TIMED: “Thermosphere Ionosphere Mesosphere Energetics and Dynamics” –NASA mission to study “the influences of the Sun and humans on the Mesosphere and Lower Thermosphere”, equipped with the SABER sensor, among others.

SABER: “Sounding of the Atmosphere using Broadband Emission Radiometry” –the sensor which acquires a column of atmospheric data via limb scanning, as part of the TIMED satellite mission

MATLAB: “Matrix Laboratory” –the coding platform which shall be used for this project.

NetCDF: “Network Common Data Form” –format for the SABER data files, as they are downloaded from the <http://saber.gats-inc.com/data.php>

NASA: “National Aeronautics and Space Administration”

NOAA: “National Oceanic and Atmospheric Administration”

Abstract

Two methods of measuring satellite via remote sensing are compared using averaged distributions of monthly collected data; a method to directly observe the infrared emission from the ozone molecule, and a proxy method from ozone dissociation by ultraviolet light. A script is written to sort the profiles of ozone into grouped bins that vary by latitude. By representing the distributions of the averaged ozone profiles graphically by hemisphere, a clear difference in the amount of ozone is shown below 90 kilometers in altitude, with higher values of ozone reported by the direct method. When comparing these averaged profiles with a photochemical model, it is found that below 60 kilometers in altitude, the direct infrared method more closely matches the model, while the model more resembles the photolysis method in the altitude region from 60 to 80 kilometers.

Introduction

The goal of this investigation was to gain a better understanding of the effectiveness of remotely sensing ozone content in the atmosphere. This was done by examining emitted near-infrared radiation from energized molecular oxygen produced via ozone photolysis, and comparing it to the infrared light emitted from ozone itself, found at its strong spectral line at 9.6 micrometers, achieved through a measure of radiance and an accompanying radiative transfer model. Ozone plays a key role in absorbing ultraviolet light from the Sun, thus heating the atmosphere. It follows that accurately measuring and creating models that represent the amount of ozone in the atmosphere is vital to understand the temperature and dynamics in the mesosphere and the lower thermosphere. By considering the strengths of different methods of remotely sensing ozone levels, a clearer image and understanding of this region can be acquired with further ease, aiding future considerations to those looking to utilize knowledge about the amount of ozone in the atmosphere.

This project will be contributing to the larger mission of the Thermosphere Ionosphere Mesosphere Energetics and Dynamics (TIMED) satellite, with its Sounding of the Atmosphere using Broadband Emission Radiometry (SABER) instrument. SABER uses two methods to detect ozone in the atmosphere: infrared radiation and near-infrared radiation detection from photolysis. This detection of ozone is achieved through a method known as limb sounding: a vertical profile of infrared radiation is acquired from scanning the Earth's limb in several different spectral intervals, chosen based on specific molecular emission features. By additionally measuring radiance along the limb, the profiles of infrared radiation measured by SABER are analyzed with the radiative transfer equation. Vertical profiles of ozone, temperature, and pressure are then derived from this.

The satellite's observation range is, daily, between the 53 degree north and 83 south latitude lines. Every 60 days the spacecraft then rotates to keep SABER pointing away from the Sun, thus alternating between the north and south hemispheres for two month intervals at a time. TIMED has been taking data for 17 years total, and has an array of datasets measured by the SABER instrument. The main question here is if the ozone measurements differ, and if so, under what conditions, and to what extent.

The expectation is that these measurements are equivalent, or of negligible difference. The satellite takes these quantities moments apart, so over any significant period, these average differences should only vary little, if at all. This variance will be quantified in a percent difference to the average of the two measurements. Thus, any difference in these averages would lend themselves to a discrepancy with how each method measures ozone. In this case, because the proxy method via photolysis requires sunlight, any profile in the intervals being averaged will be from a range where the ozone is in equilibrium that is not changing rapidly in time. So, it is necessary to only examine profiles a certain amount of time after sunrise, and before sunset. In order to compare these measurements, primarily with model calculations, monthly averages of the ozone data are computed.

Physical Theory to be Modeled

The first principle to be modeled is found by looking at the products of ozone being separated in a process known as photolysis. Ozone absorbs solar ultraviolet radiation in the Hartley band (with a wavelength of 220-310 nm) and is dissociated into molecular and atomic oxygen, producing them in excited states. The molecular oxygen is produced in its lowest lying

state, $O_2 (^1\Delta)$, which then radiates strongly at a wavelength of 1.27 micrometers. The amount of this excited O_2 is also reduced in collisions with oxygen and nitrogen gas, to which there exists a detailed model of this $O_2 (^1\Delta)$ state that relates the observed near infrared emission from $O_2 (^1\Delta)$ to the amount of ozone in the atmosphere (Mlynchak, Martin G., et al., 2007). So, by proxy of the ultraviolet light contributing to ozone photolysis, the amount of ozone in the atmosphere can be found based on the interactions of the produced excited molecular oxygen with its near infrared emissions, and interactions with available oxygen and nitrogen.

For example, if the photolysis rate of ozone is denoted by J , the $O_2 (^1\Delta)$ emission rate as A , and the collision rate with $O_2 (^1\Delta)$ and O_2 (to form 2 O_2 and release kinetic energy) as “ k ”, the time rate of change of $O_2 (^1\Delta)$ can be described as:

$$\frac{\partial O_2 (^1\Delta)}{\partial t} = J * O_3 - A * O_2 (^1\Delta) - k * O_2 (^1\Delta)$$

Which has a critical value where

$$\frac{J * O_3}{A + k} = O_2 (^1\Delta)$$

By solving the radiative transfer equation (with τ being the atmospheric transmittance), the measured radiance can be utilized with the known gradient of transmittance along the limb and the source function S (a function of $O_2 (\Delta)$):

$$R = \int S * \frac{\partial \tau}{\partial x} * dx$$

Deriving the amount of $O_2 (^1\Delta)$ from S and calculating the photolysis rate, J , the amount of ozone can be calculated:

$$J * O_3 = (A + k) O_2 (^1\Delta)$$

Where J, A, and k have been experimentally determined, and $O_2 (^1\Delta)$ is derived. This value for ozone expressed in terms of a mixing ratio—a value representing the number of ozone molecules detected, divided by the number of particles in the atmosphere (the data will show this value in parts per million when examining the distribution along the altitude range examined).

The other principle used to measure ozone is to directly observe the infrared emission from the ozone molecule, which has a strong absorption band at 9.6 micrometers. Measurements of this emission in the atmosphere, coupled with simultaneous measurements of temperature and pressure made by observing CO₂ emission with SABER at 15 micrometers, allow the ozone amount to be derived, using the same radiative transfer techniques, with the exception that S is replaced with the Plank function (a function of temperature).

Both SABER data sets contain ozone levels over the same latitude, altitude, and time ranges—the data will be limited to the satellite’s maximum latitude range for continuous, year-round observations, of roughly 50 degrees north and south. That will be the starting point to understand how the datasets couple with theory on how ozone levels vary over time in cyclic patterns. Percent differences to the average and distributions of ozone level measurements with a solar zenith angle of no more than 60 degrees, and groupings within latitude ranges of 5 degrees will be collected. The zenith angle requirement is necessary to ensure the system is in a state known as steady daylight conditions—the $O_2 (^1\Delta)$ molecules in large take time to radiate the energy from their excited state, in a period of about 75 minutes. By waiting until the sun has reached a certain angle to the normal of the surface, the conditions that ozone is being measured

would not differ due to a delay via the proxy method, strengthening the comparison of the processes with each other.

Methods

The data being worked with has been taken by SABER for the past 17 years, and it is specifically its two methods of measuring ozone that are being examined. Using a feature known as the custom data tool on the website for accessing this data (found at: <http://saber.gats-inc.com/data.php>), four “options” can be selected for what the user wants. The two measurement methods are found in O3_96 and O3_127, atmospheric pressure is standard for any configuration of the data tool, and temperature (in kelvin) is included for the 9.6 micron method. The year studied will be the satellites first year of steady data, 2004. Starting with December 2003, each month will be averaged for both methods, with the same 40 to 100 kilometer altitude range for all cases. Latitudes will be taken up to 50 degrees North and the 50 degrees South. This region is continuously observed by the satellite—latitudes further poleward may be excluded when the satellite shifts hemisphere after two months.

These datasets will directly interact with the coding platform, chosen to be MATLAB for this project. To understand and visually inspect the data an additional script (detailed in the component specifications section) will be used to translate the NetCDF files to American Standard Code for Information Interchange (ASCII) text files, containing tables of information according to each of the parameters selected with the custom data tool. For the main part of this project, monthly averages for altitudes partitioned over the range the data taken will be computed from the SABER data files. These files will be directly called within MATLAB, and the final product should be able to cycle through years of data to extract these monthly averages.

The second major choice made was MATLAB, as opposed to other coding platforms. Aspects of this that are useful are its ability to read the NetCDF files, capacity to translate into ASCII, capability to perform the type of sorting work required when making the script for the product (see the component specifications), and the statistical toolkit mod that adds functions that can be used to analyze the results of the monthly averages. The main competition for this platform was IDL. While it could perform the work needed, MATLAB was made available to no cost, and even if it wasn't, the un-modded version of MATLAB, plus the statistical toolkit, cost far less than IDL without any add-ons. Both would be new languages to learn, so the amount of work needed to perform this project would be the same. There is no evidence currently if one could read / format the files faster, so MATLAB remains at an advantage.

After these methods are compared with each other, the available winter and spring months shall also be compared to a photochemical model, which predicts what the amount of ozone *should* be along similar profiles against altitude. The values for the measurements of this model are already given, and divided into certain latitude regions. Calculated values will be averaged into the same range as the measured distributions and plotted alongside to understand how the expectation for the amount of ozone compares to those derived from the satellite data.

For the code itself, I began by getting the indices of SABER profiles that fit the steady daylight range. These profiles have elements down their column correlating to altitude measurements. Instead of considering each element in a column individually, a single element—halfway through the range of altitude values—will be used to characterize the entire profile. The latitude and solar zenith angle of this element in the profile can then be marker for which that profile is sorted into the corresponding bin. If the solar zenith angle is within the required range, the profile is then sorted by latitude, mathematically adding the profile to the sum of prior

profiles in that latitude bin. After this is done, the average of the profiles is taken to return the monthly average. This averaging process is repeated for the photolysis and infrared method up to the 45 degrees North bin (whose upper limit is 50 degrees North). Each table is then saved to a structure, which can be opened and called from in order to continue to the next step of analysis.

Data

In order to display the information gathered through the SABER dataset, the tables that been averaged previously would be collected into averages in the northern and southern hemisphere. For each month in 2004, the mixing ratios and altitudes for each method are averaged in every table that has available data in the hemisphere range.

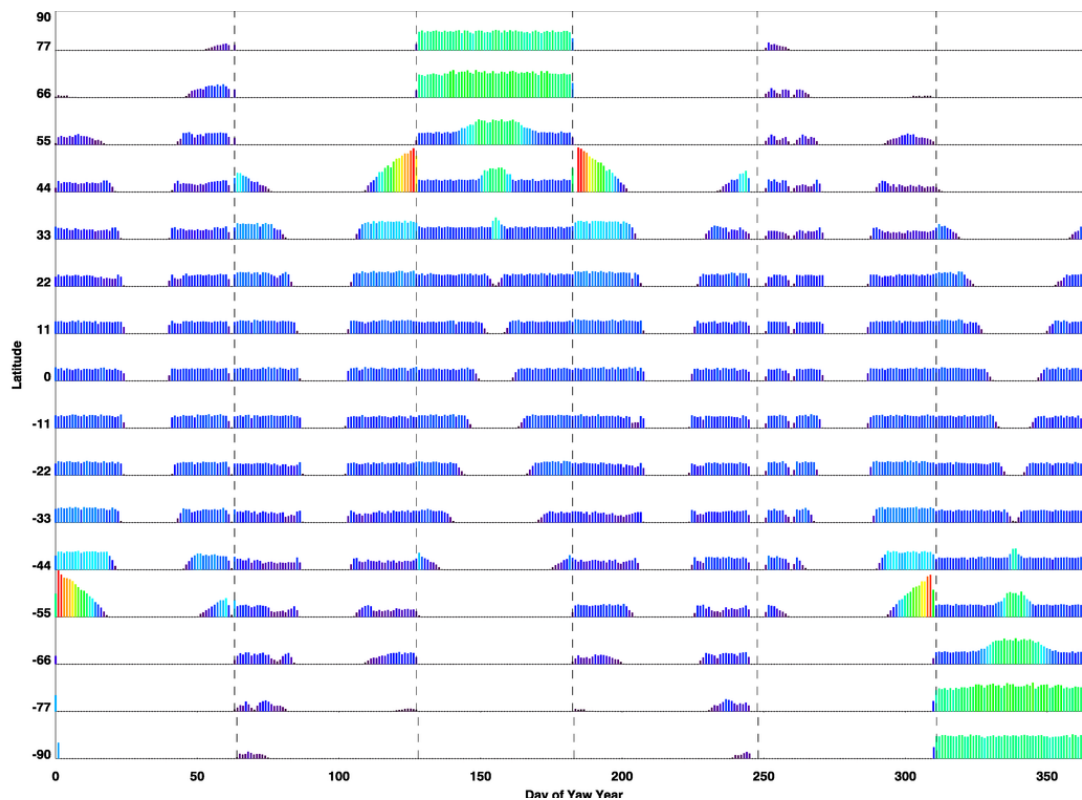


Figure 1: SABER day observations by yaw cycle and latitude. Note that the day of the year axis shows the lack of profiles taken during the daytime in February, April, August, and October.

As seen in Figure 1, there are several days during the year when the instrument does not observe during the daytime; only nighttime profiles are available at these points, but the photolysis method cannot be compared to the infrared method in these months as the satellite is not seeing the ozone dissociation on the daytime side of Earth. This gathered information will display an average of all available information in the steady daylight range, and the results will be drawn from both the distributions of the two methods, and the percent difference the mixing ratios in those distributions have with each other, with respect to the average of those two ratios. For each month, four figures will be plotted: a distribution and a percent difference plot for both hemispheres.

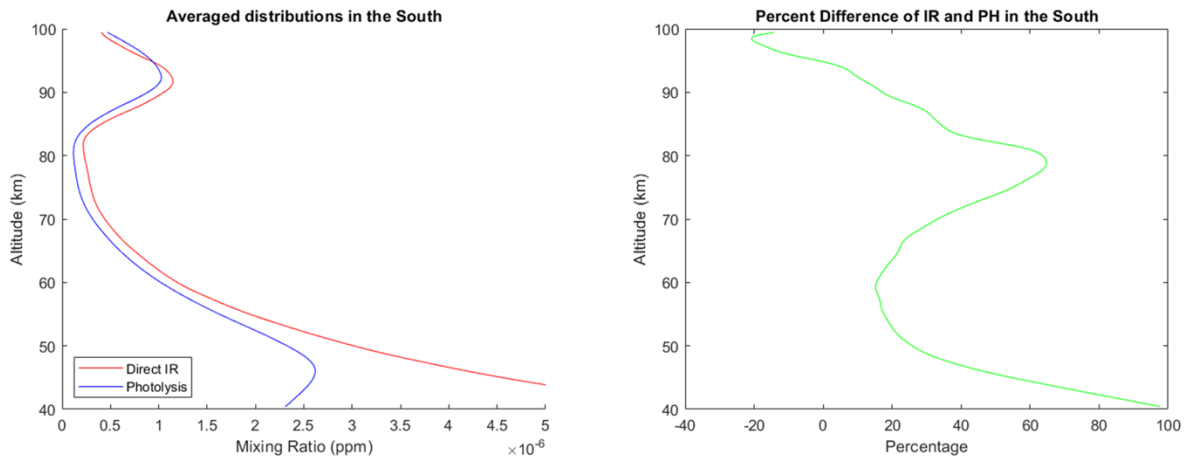


Figure 2: Computed averages and percent differences for December of 2003

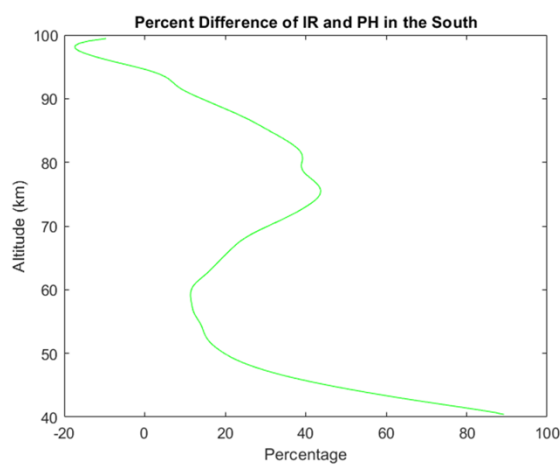
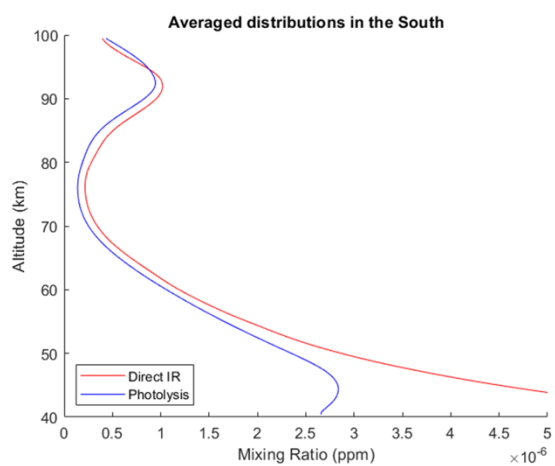
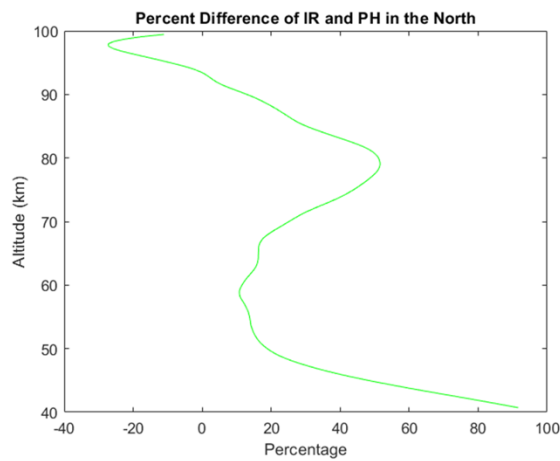
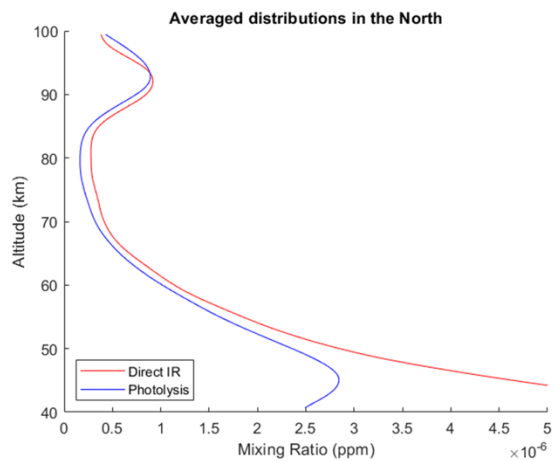
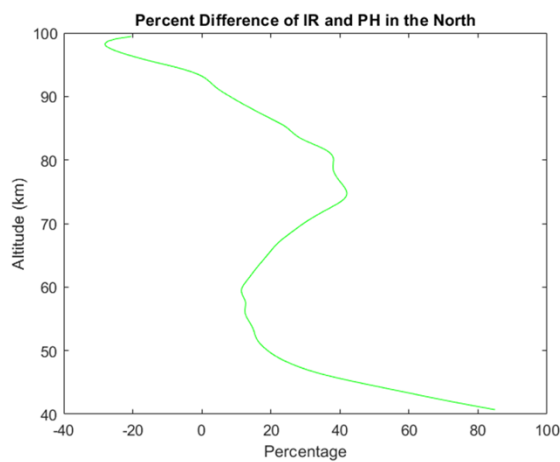
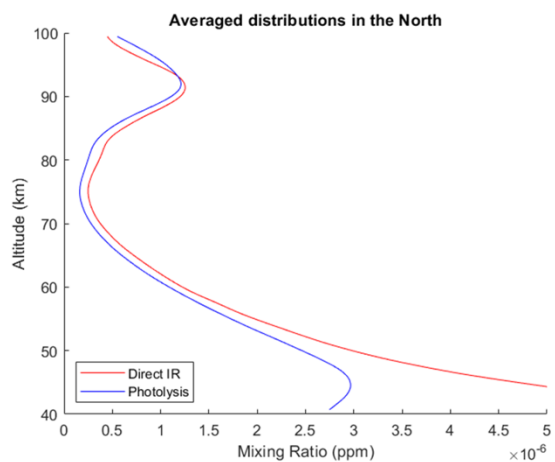


Figure 3: Computed averages and percent differences for January of 2004



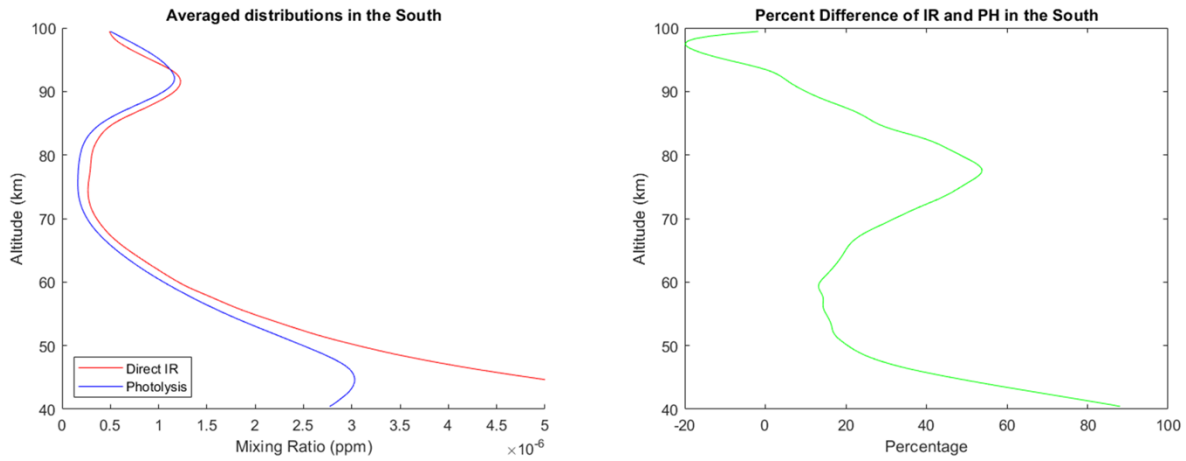


Figure 4: Computed averages and percent differences for March of 2004

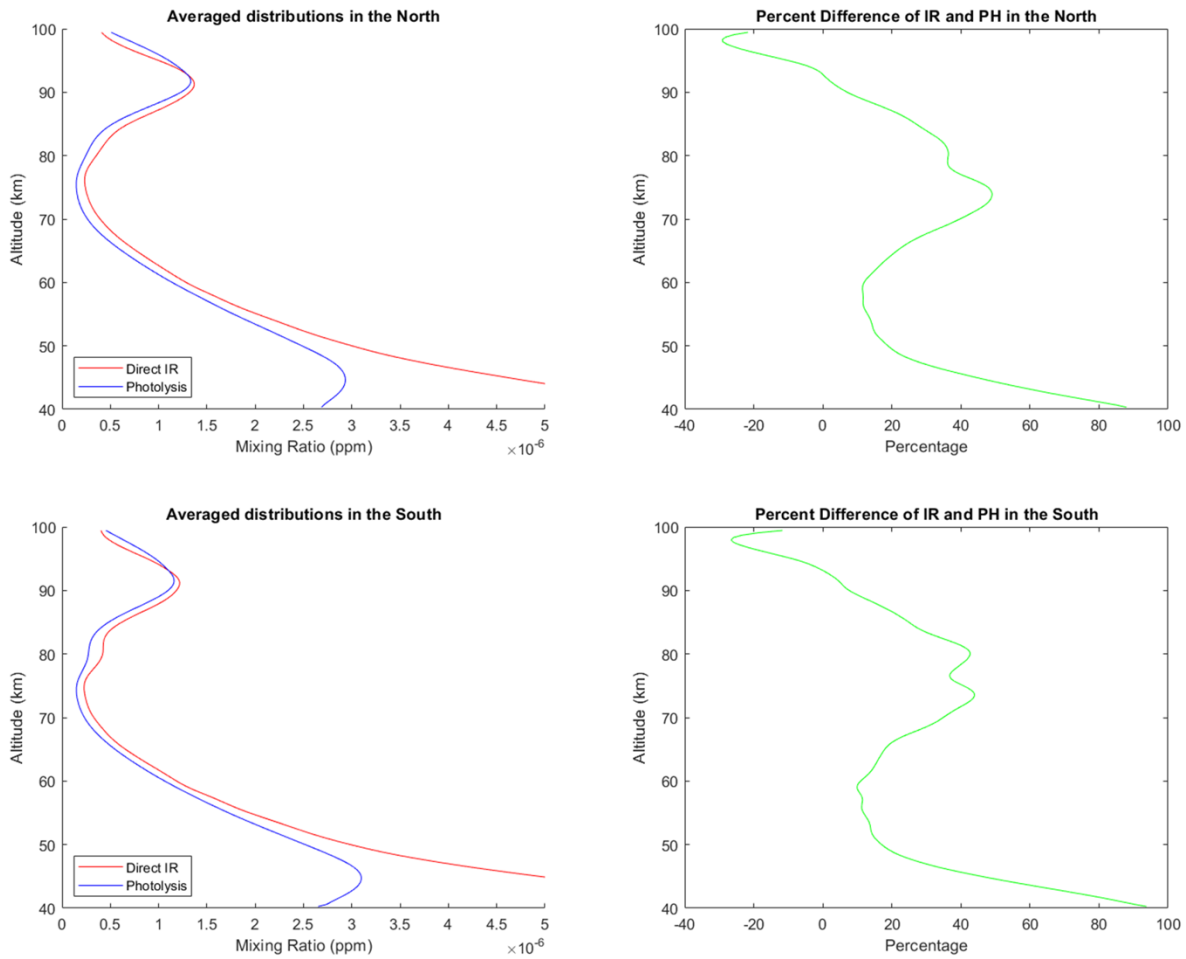


Figure 5: Computed averages and percent differences for May of 2004

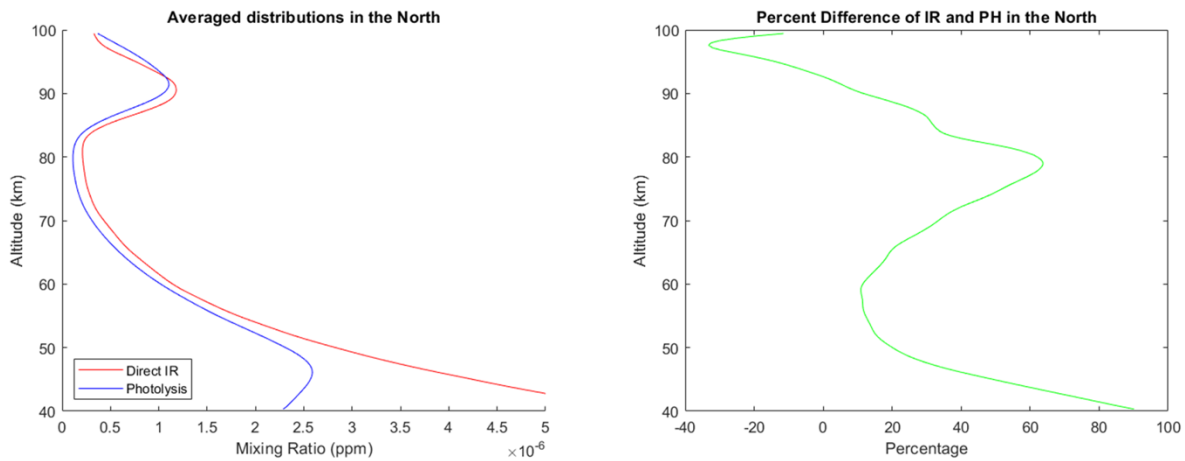


Figure 6: Computed averages and percent differences for June of 2004

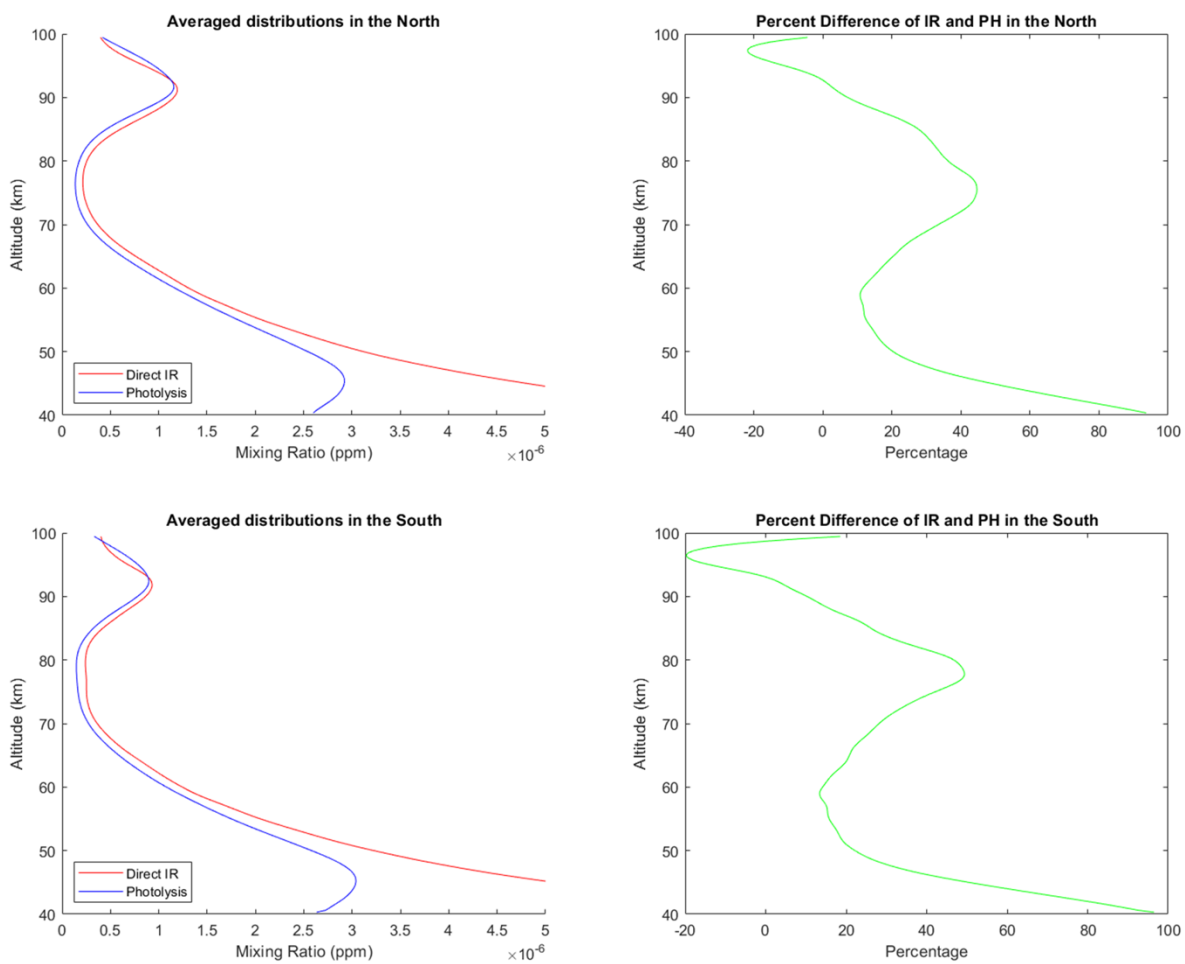


Figure 7: Computed averages and percent differences for July of 2004

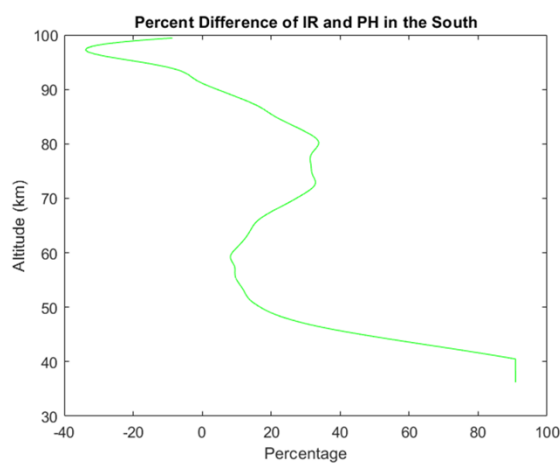
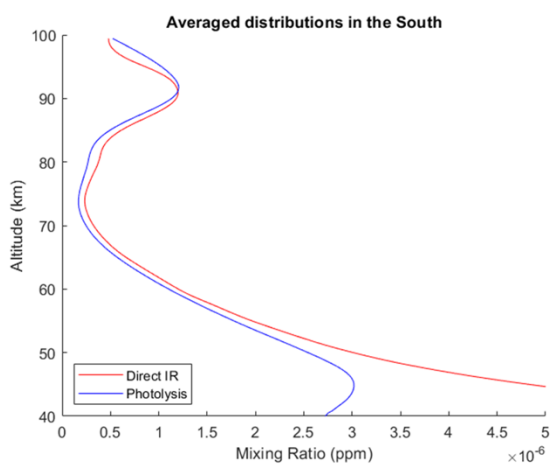
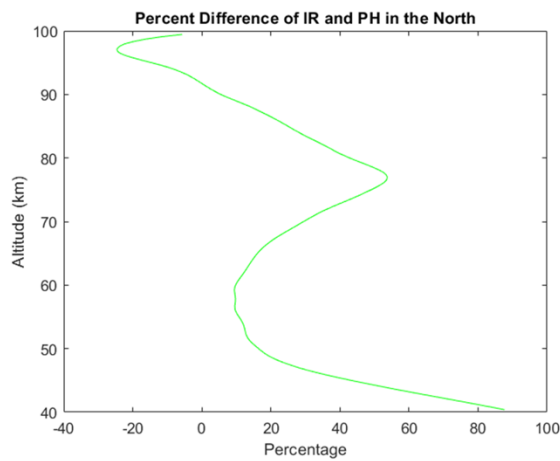
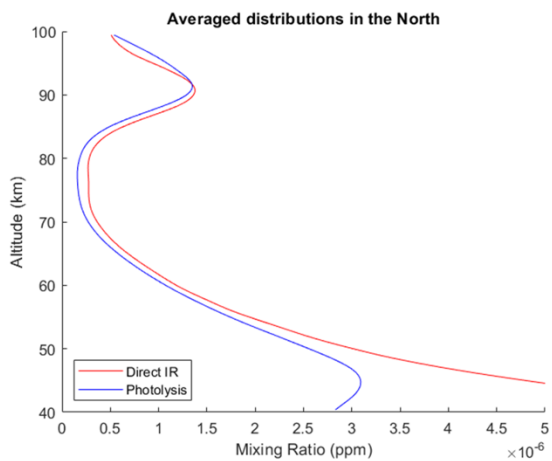
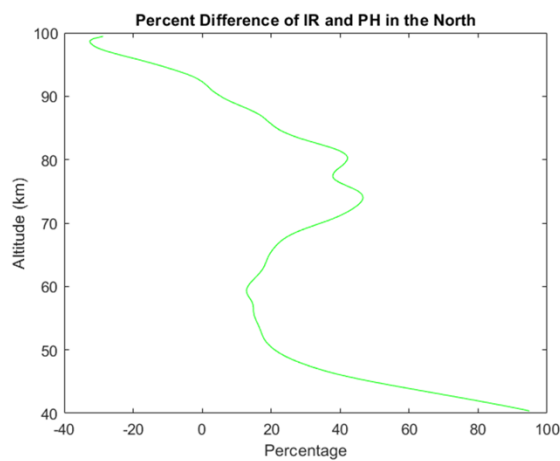
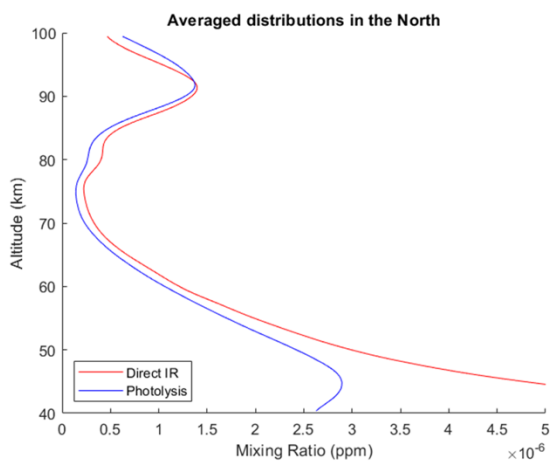


Figure 8: Computed averages and percent differences for September of 2004



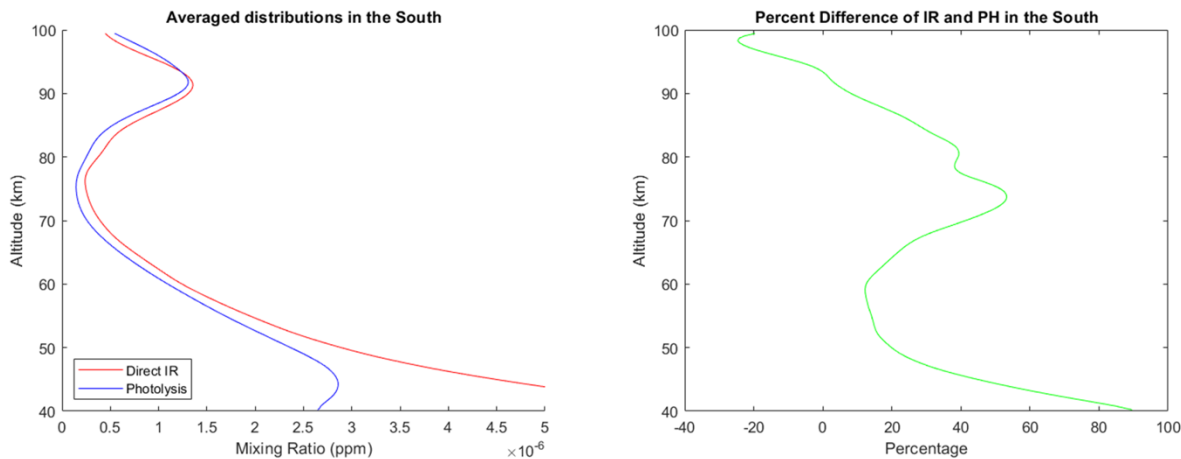


Figure 9: Computed averages and percent differences for November of 2004

Additionally, the following months include the photochemical model averages for those hemispheres:

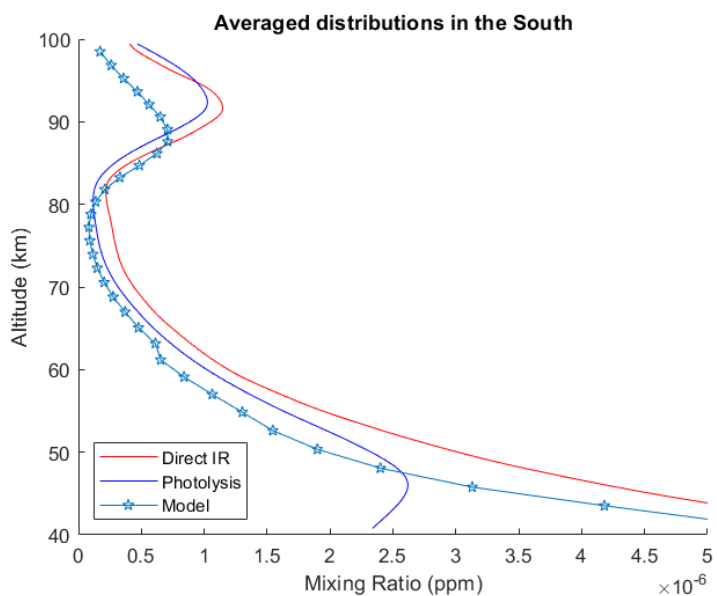


Figure 10: Computed averages with photochemical model for December of 2003

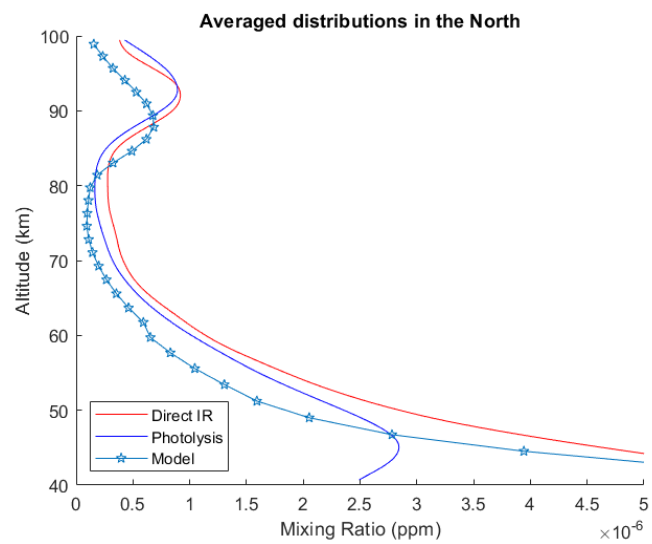


Figure 11: Computed averages with photochemical model for January of 2004 (Northern hemisphere)

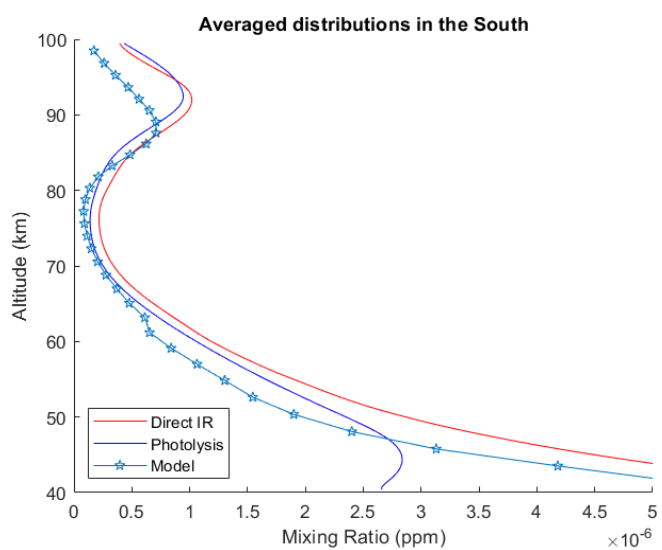


Figure 12: Computed averages with photochemical model for January of 2004 (Southern Hemisphere)

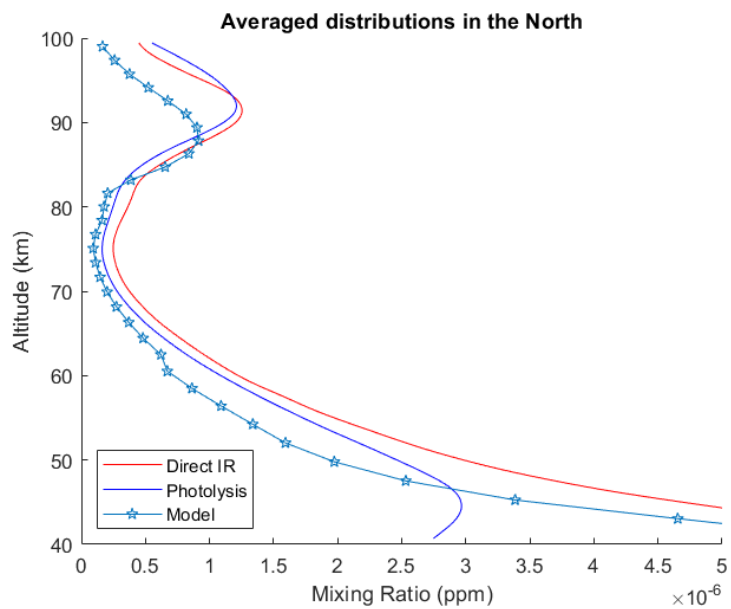


Figure 13: Computed averages with photochemical model for March of 2004 (Northern Hemisphere)

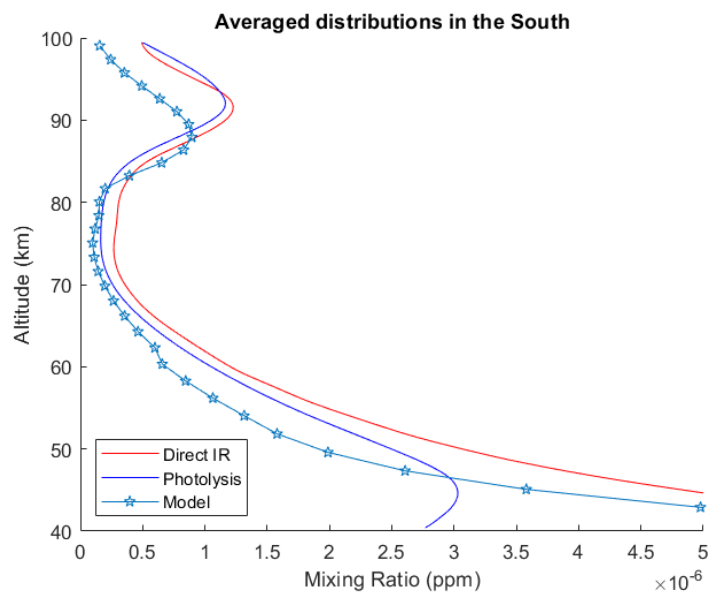


Figure 14: Computed averages with photochemical model for March of 2004 (Southern Hemisphere)

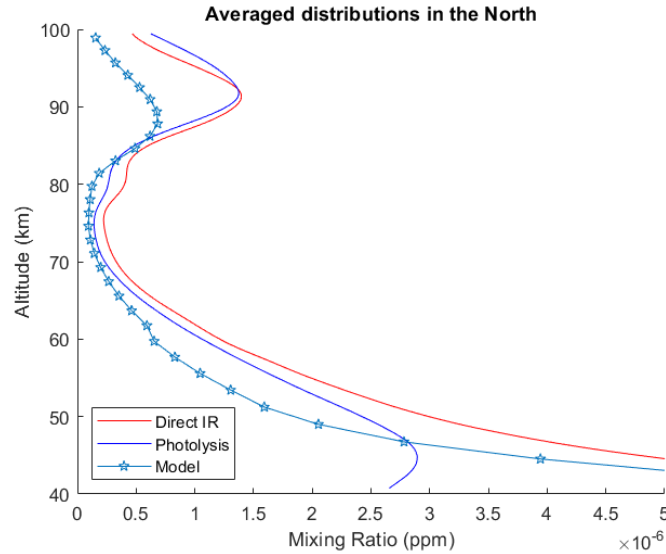


Figure 15: Computed averages with photochemical model for November of 2004 (Northern Hemisphere)

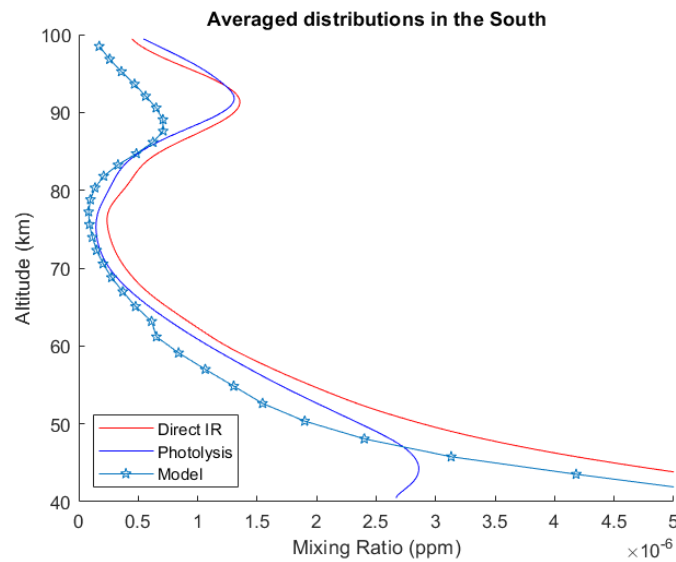


Figure 16: Computed averages with photochemical model for November of 2004 (Southern Hemisphere)

As seen in both the northern and southern hemispheres, in every month above, the direct infrared method of measuring ozone consistently reports higher values for the mixing ratio of ozone than compared to the proxy photolysis method, under altitudes of 90 kilometers. The percent difference between these methods thus varies from zero to over 100 percent, in cases such as December. There is a local maximum in the difference in areas where the distribution meets a local minimum, quite possibly due to the fact that the percent difference is calculated

with respect to the average of the two methods. Of note, the difference plot reaches a local minimum soon after, as the mixing ratio increases as expected for gases at lower altitude.

Discussion and Conclusions

The result of the data went against the expectation that there would not be a clear bias in measurement for either method, as the amount ozone would not change when a profile is taken for both methods. Furthermore, this bias is not immediately dependent on location and the time of year, as the result holds for each hemisphere of every month. The only difference that the time of year makes is the altitude at which an intersection occurs between the distributions of the two mixing ratios; however, given how sparse gases are at these altitudes, it is suspected that this is a result of a weak signal to noise ratio in that region. Further work must be done to verify if this is indeed an artifact of high altitudes, or indeed something that varies with constraints, such as location.

This result supports the prior findings of a study on Satellite observations of ozone in the upper mesosphere (Smith et. al.). When comparing the datasets of similar methods across several different satellite sensors—including TIMED’s SABER sensor—they found that SABER’s 9.6 micrometer measurement recorded higher values than the others: “Ozone from the SABER 9.6 μm channel is higher than the other measurements over the altitude range 60–80 km by 20–50%”, which would agree with the averaged sets (Smith et. al.). In the averaged data shown previously, altitude range contains a local maximum the percent difference, which agrees with Smith et. al.. The direct infrared method is still approximately 10% greater than the photolysis method in all cases, and that difference only increases the lower in altitude from there.

It is suspected that the intersection at upper altitudes is due to a weak signal to noise ratio in that region, possibly in combination to the differences in the methods used to derive ozone at lower altitudes. Because there is less radiance from that point, less ozone is derived from it (Smith et. al.).

For the photochemical model calculations, several conclusions can be drawn when comparing them to the distributions for the spring and the winter. Firstly, below the 60 kilometer altitude, the model follows the distribution of the infrared readings, despite reporting lower values. The chemical model does not decrease in value like the photolysis method does at the lowest altitudes, indicating that below the 60 kilometer line, the infrared readings match more closely to what the model predicts is the correct general shape of the distribution. Next, between 60 and 80 kilometers, the model closely resembles the ozone derived from the photolysis method, even approaching in value. This indicates that the photolysis method measures a distribution that would be predicted by this model. Lastly, the model contrasts with the averaged measurements at the “secondary maximum”, capping at roughly half as much in parts per million as what the direct infrared and the proxy photolysis methods report.

Because the two methods of measuring ozone differ significantly, and that difference isn’t isolated to a seasonal hemisphere difference, or that of altitude, there are new directions opened in going forward. Foremost is to see if this trend continues in following years. The product that was coded in the solution to this project is easily adaptable to this end, simply running and plotting additional years. While this describes how the two approaches to remotely sensing ozone vary, it gives little indication alone as to what is the more accurate result to the true amount of ozone; although, the photochemical model could be used to isolate parts of the distribution to further explain how these methods differ. Further investigation could also be

directed at the intersection points in the upper altitude region of the distributions, to see why the infrared method is consistently reading lower than the photolysis in that 3-4 kilometer range. This study also does not answer why the photolysis method curves away from the expected values for the mixing ratios at lower altitudes, instead favoring a lower, as opposed to a higher ratio. Instead of a two-step averaging process, tropical and mid-latitude bins could be created to make a similar comparison, instead of a hemisphere of 5 degree bins.

Appendix:

- For the functionality of the code, SABER NETCDF files were renamed to a “month_year” format to aid in the fetching of data, and the save file that is created once the averages are done.

Formal Citations

- Mlynczak, Martin G., et al. "Sounding of the Atmosphere Using Broadband Emission Radiometry Observations of Daytime Mesospheric O₂(1Δ) 1.27μm Emission and Derivation of Ozone, Atomic Oxygen, and Solar and Chemical Energy Deposition Rates." *Journal of Geophysical Research*, vol. 112, no. D15, 2007, doi:10.1029/2006jd008355.
- Mlynczak, M. G., and S. Solomon (1991), On the efficiency of solar heating in the middle atmosphere, *Geophys. Res. Lett.*, 18, 1201– 1204.
- Mlynczak, M. G., S. Solomon, and D. S. Zaras (1993), An updated model for O₂(a1Dg) concentrations in the mesosphere and lower thermosphere and implications for remote sensing of ozone at 1.27 mm, *J. Geophys. Res.*, 98, 18,639– 18,648.
- Smith, A. K., et al. (2013), Satellite observations of ozone in the upper mesosphere, *J. Geophys. Res. Atmos.*, 118, 5803– 5821, doi:10.1002/jgrd.50445.